

Kinetic analysis of the catalytic pyrolysis of Jimsar oil shale with $\text{CoCl}_2 \cdot 6\text{H}_2\text{O}$

Ni Pan*, Liang Zhou

The State Key Laboratory of Refractories and Metallurgy, Wuhan University of Science and Technology, No. 947 Heping Avenue, Qingshan District, Wuhan 430081, PR China

Received 1 October 2021, accepted 22 April 2022, available online 10 June 2022

Abstract. *In this paper, the catalytic pyrolysis of Jimsar oil shale was studied using $\text{CoCl}_2 \cdot 6\text{H}_2\text{O}$ as a catalyst. The thermogravimetric analysis (TGA) was carried out on oil shale samples with the catalyst added. The kinetic analysis of the pyrolysis reaction of each sample was performed using the main curve method and several model-free methods. The results showed that $\text{CoCl}_2 \cdot 6\text{H}_2\text{O}$ could not only reduce the average activation energy of oil shale pyrolysis from 216 kJ/mol to 163 kJ/mol, but also decrease the pyrolysis temperature by about 100 °C.*

Keywords: *Jimsar oil shale, thermogravimetric analysis, catalytic pyrolysis, kinetic analysis.*

1. Introduction

The pyrolysis of oil shale is a very complex thermophysical chemical process which is affected by many factors, such as reaction temperature, particle size, high temperature residence time, catalyst and mineral content. Catalyst can influence the rate of reaction without changing the total Gibbs free energy further. Therefore, when studying conventional pyrolysis of oil shale, scholars have also conducted extensive research on its catalytic pyrolysis, with the aim to find a cheaper and more practical catalyst, reduce the energy consumption of the pyrolysis process, raise the transformation rate of organic matter pyrolysis, increase the production of shale oil and gas and reduce the cost of production.

Pyrite [1–3] and transition metal salts [4, 5] have become the focus of scholars all over the world. It can be seen from the relevant literature that

* Corresponding author: e-mail pennyup@126.com

catalysts can indeed improve the oil recovery rate of oil shale, but different catalysts possess different catalytic effects, while the same catalyst can have different catalytic effects on oil shales from different regions.

Reaction kinetics can accurately describe the process of a reaction, so mastering each reaction's kinetic parameters can help researchers control this process, which is the theoretical guidance for industrial production. When studying the pyrolysis kinetics of Jimsar oil shale, Pan [6] calculated the activation energies at different conversion rates by means of the equal conversion rate method, and deduced the oil shale reaction mechanism. However, the pyrolysis of oil shale is a very complex process, there may take place multiple competing or parallel reactions, and between the reaction products there occurs a secondary reaction [7–10]. Also, based on the recommendations of the International Confederation for Thermal Analysis and Calorimetry (ICTAC), Vyazovkin et al. [11] suggest that complex multi-step reactions should be completely separated and the respective kinetic parameters should be analyzed. The focus is on the pyrolysis of oil shale, whose organic matter is mainly composed of asphalt and kerogen. Based on an earlier study on the influence of transition metals on the pyrolysis of Jimsar oil shale [12], this paper investigates the kinetic parameters in its catalytic pyrolysis process, to grasp the reaction process further, and provide the theoretical support for industrial production. This article assumes that there are two main parallel pyrolysis processes of organic matter: the thermal evaporation of asphalt and the pyrolysis of kerogen. The kinetic parameters of each sub-reaction and the whole reaction are studied to understand the pyrolysis mechanism of Jimsar oil shale more thoroughly.

2. Material and methods

The theoretical foundations in this study are similar to those used before [13].

2.1. Oil shale samples

The oil shale samples used in this study were obtained from Jimsar, Xinjiang Province, northwestern China. The characteristics of the oil shale are given in Table 1.

Table 1. Characteristics of raw oil shale sample, wt%

C_d , %	H_d , %	O_d , %	N_d , %	$S_{t,d}$, %
16.03	1.81	3.69	0.7	0.57

d – dry basis; t – total

2.2. Experimental procedure

The thermogravimetric/differential thermal-mass spectrometric (TG/DT-MS) analyses were carried out using a Netzsch STA 449 f3 analyzer. About 10 mg samples were distributed uniformly in the crucible and heated from ambient temperature to 1000 °C at a heating rate of 5, 10, 15 and 20 °C/min. The flow rate of argon as carrier gas was maintained at 60 ml/min during the whole experimental process. The derived products were swept into a mass spectrometer through the capillary column connected with the TG analyzer. The temperature of the capillary was kept at 255 °C to avoid plugging. The weight loss of the sample was continuously recorded as a function of temperature and time through the TG analyzer during the pyrolysis process.

3. Results and discussion

Four TG-MS analyses of OS-Co samples at different heating rates were carried out, the TG contrast curve is shown in Figure 1. It reveals that the heating rate has little influence on the pyrolysis process. However, with the increase of heating rate, the pyrolysis reaction moves to the high temperature zone as a whole. Figure 2 shows the differential thermogravimetric (DTG) curves of OS-Co samples at different heating rates. It can be seen that with the increase of heating rate, the range of pyrolysis temperature increases and the peak temperature at each stage moves towards high temperature, which is caused by the temperature gradient inside the sample particles.

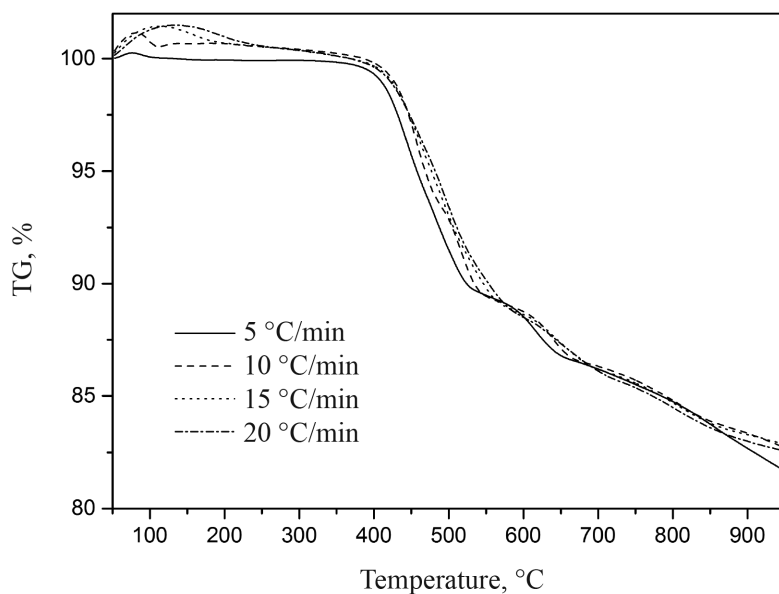


Fig. 1. TG curves of OS-Co samples at different heating rates.

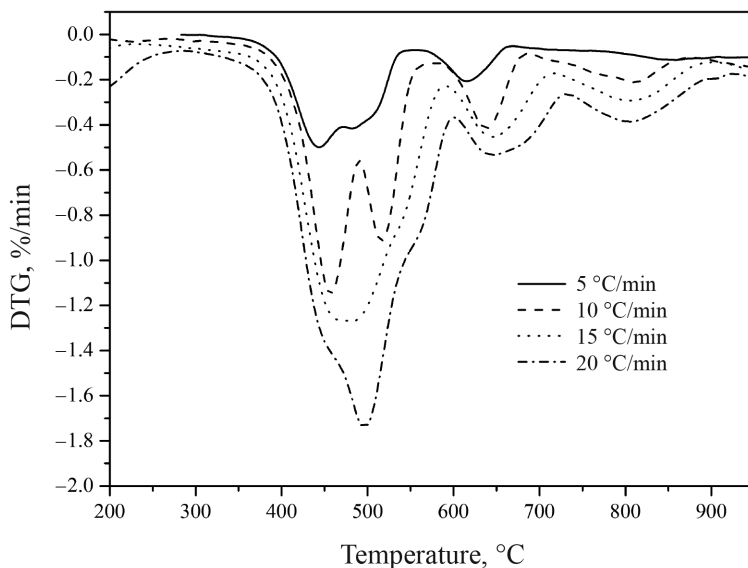


Fig. 2. DTG curves of OS-Co samples at different heating rates.

Figure 3 shows the Bi-Gaussian multi-peak fitting curves of OS-Co samples at different heating rates. The figure reveals that at a low heating rate, the pyrolysis around 550 °C can be divided into two stages, in which the lower temperature stage is dominated by the pyrolysis of organic matter, while the higher temperature stage is still considered as the pyrolysis stage of inorganic minerals. However, with the increase of heating rate, the temperature range corresponding to the two reaction stages increases, and the peak temperature increases. At the same time, there is an overlapping region between the two stages, and the area of this region increases with the increase of heating rate. The sub-reactions were successively named as Reaction I, Reaction II, Reaction III and Reaction IV, among which Reaction IV represents the pyrolysis reaction of inorganic mineral salts.

Two main curve methods were used to analyze the subpeaks shown in Figure 3. It was found that the standard curve based on the integral form had no reaction mechanism function consistent with the experimental curve. The analysis results of the main curve method based on integral and differential forms are shown in Figure 4. It can be seen from the figure that Reaction I and Reaction III can be described by the F_2 function, while Reaction II and Reaction IV can be described by the $D\text{-ZLT}_3$ function. According to the analysis results of OS-R samples, the two sub-reactions of organic matter can be described by F_2 and $D\text{-ZLT}_3$, respectively. Therefore, we believe that Reaction III of the OS-Co sample is an inorganic mineral salt reaction advanced by the influence of $\text{CoCl}_2 \cdot 6\text{H}_2\text{O}$ catalyst, which is adjacent to and partially overlaps with Reaction IV.

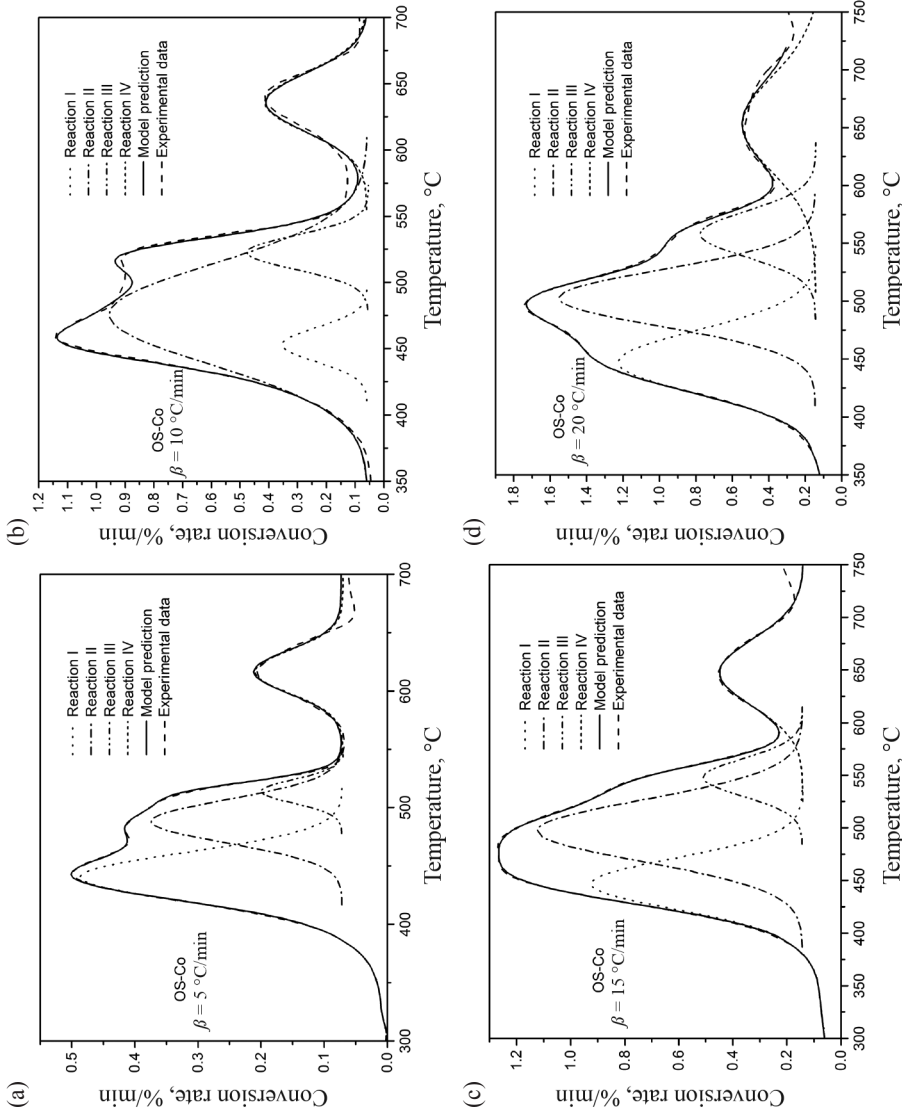


Fig. 3. Bi-Gaussian multi-peak fitting for OS-Co at varying heating rates: (a) at $\beta = 5\text{ }^{\circ}\text{C}/\text{min}$; (b) at $\beta = 10\text{ }^{\circ}\text{C}/\text{min}$; (c) at $\beta = 15\text{ }^{\circ}\text{C}/\text{min}$; (d) at $\beta = 20\text{ }^{\circ}\text{C}/\text{min}$.

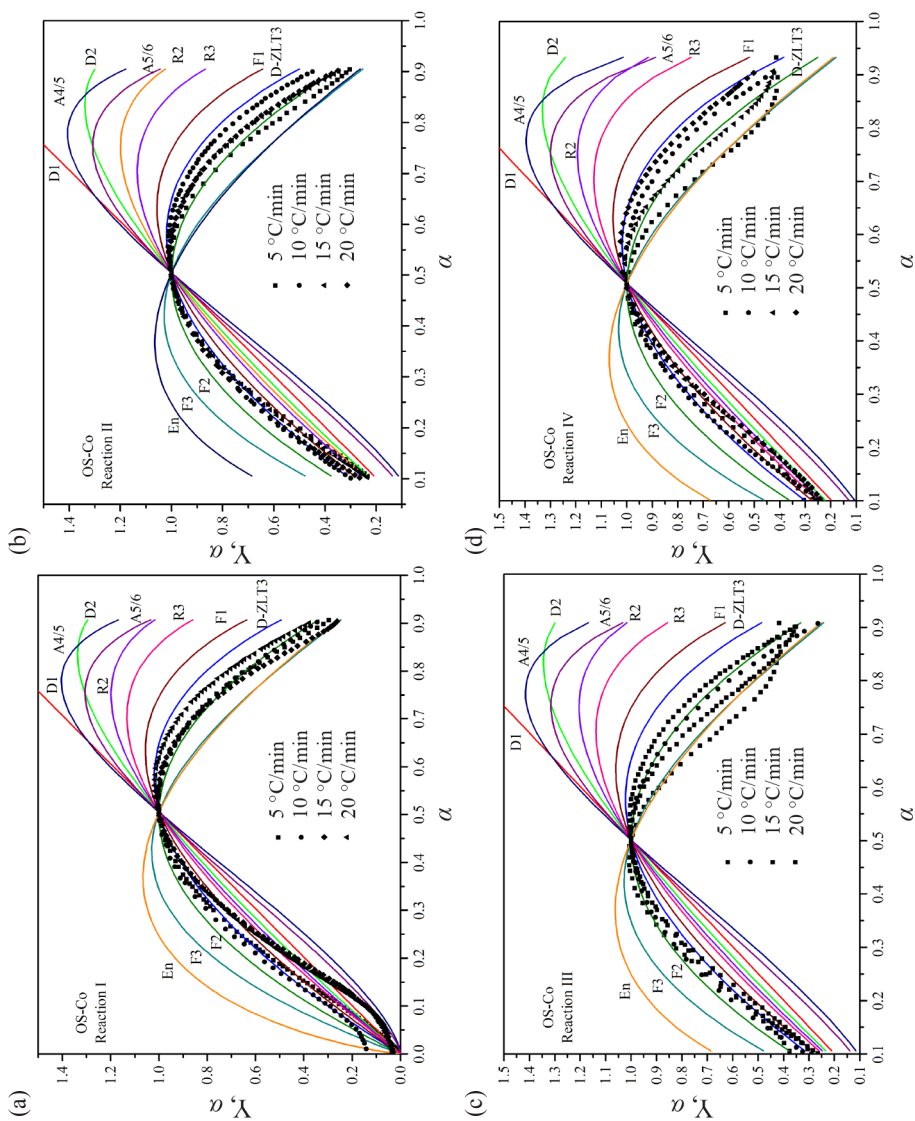


Fig. 4. (a)–(d) Contrast between experimental results and a standard $Y(\alpha)$ plot.

On the basis of a multi-peaks Bi-Gaussian fitting, three methods of activation energy calculation were used to calculate the activation energy values of each sub-reaction and the main stage. The results are shown in Figure 5 and Table 2.

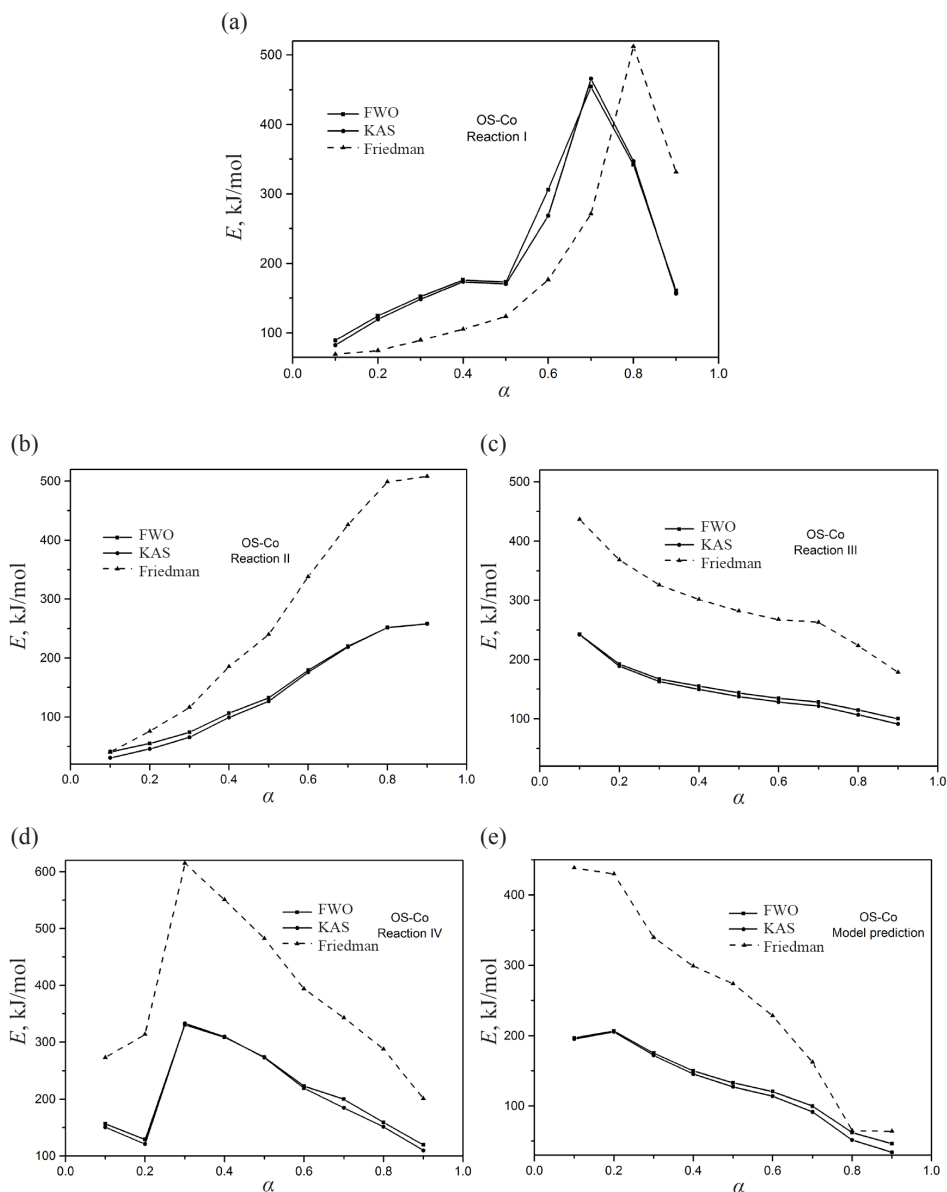


Fig. 5. Relationship between the activation energy and conversion rate of OS-Co samples at different stages and sub-peaks: (a) comparison of activation energies of Reaction I calculated by different methods; (b) comparison of activation energies of Reaction II calculated by different methods; (c) comparison of activation energies of Reaction III calculated by different methods; (d) comparison of activation energies of Reaction IV calculated by different methods; (e) comparison of activation energies of the fitting curve fitting curve calculated by different methods.

Table 2. Kinetic triplets of sub-reactions for the OS-Co oil shale sample

Stage	β	T_{\max}	\bar{E}	Mechanism		lnA
				Function	R	
Reaction I	5	440	195	F_2	0.9873	29.89
	10	452			0.9852	33.19
	15	446			0.9815	34.78
	20	447			0.9847	35.5
Reaction II	5	487	144	D-ZLT ₃	0.9768	23.18
	10	475			0.9877	23.94
	15	497			0.9676	24.08
	20	503			0.9748	24.47
Reaction III	5	513	150	F_2	0.9816	20.86
	10	522			0.9873	25.55
	15	547			0.9884	25.4
	20	558			0.9858	25.85
Reaction IV	5	616	208	D-ZLT ₃	0.9863	27.57
	10	636			0.9847	27.15
	15	647			0.9858	27.33
	20	653			0.9876	28.03

It can be seen from the figure that the results of FWO and KAS methods are in good agreement, while the change trend of activation energy calculated by the Friedman method is the same as that of the other two methods, but the values differ greatly. By comparing the pyrolysis activation energy of OS-Co and OS-R samples, under the catalysis of $\text{CoCl}_2 \cdot 6\text{H}_2\text{O}$, the reaction activation energy is significantly reduced, which means that the energy required for the reaction is reduced and the reaction temperature is lowered. As can be seen from the change trend of activation energy with conversion rate, for organic matter, the higher the conversion rate, the higher the activation energy, while for inorganic minerals, the initial reaction maximum activation energy decreases with increasing conversion rate.

4. Conclusions

In this paper, $\text{CoCl}_2 \cdot 6\text{H}_2\text{O}$ was used as catalyst to conduct a thermogravimetric experiment on the catalytic pyrolysis of Jimsar oil shale. The Bi-Gaussian principal peak fitting method and two kinds of the meta-curve analysis method were used to analyze the kinetic parameters of the pyrolysis process. The main conclusions are as follows:

1. The heating rate has little influence on the catalytic pyrolysis.
2. For each sub-reaction, the mechanism of Reaction I and Reaction III can be expressed by the F_2 equation, while that of Reaction II and Reaction IV can be expressed by the D-ZLT₃ equation.
3. The activation energy is greatly reduced with the addition of a catalyst.

Acknowledgements

This work was supported by the Innovation and Entrepreneurship Training Program of Hubei Province of China (Project No. S202110488006) and the Key Laboratory for Ferrous Metallurgy and Resources Utilization of the Ministry of Education of Wuhan Science and Technology.

REFERENCES

1. Bakr, M. Y., Yokono T., Sanada, Y., Akiyama, M. Role of pyrite during the thermal degradation of kerogen using in situ high-temperature ESR technique. *Energy Fuels*, 1991, **5**(3), 441–444.
2. Han, B. *Effect of Pyrite on the Pyrolysis of Organic Matter and its Semi-Coke Functional Groups in Longkou Oil Shale*. Ph.D. Thesis, Harbin Institute of Technology, 2016 (in Chinese).
3. Zhang, J. L., Zhang, P. Z. A discussion of pyrite catalysis on the hydrocarbon generation process. *Advances in Earth Sciences*, 1996, **11**(3), 282–287 (in Chinese).
4. Jiang, H. F., Song, L. H., Cheng, Z. Q., Chen, J., Zhang, L., Zhang, M. Y., Hu, M. J., Li, J. N., Li, J. F. Influence of pyrolysis condition and transition metal salt on the product yield and characterization via Huadian oil shale pyrolysis. *J. Anal. Appl. Pyrolysis*, 2015, **112**, 230–236.
5. Holstein, W. L., Boudart, M. Transition metal and metal oxide catalysed gasification of carbon by oxygen, water, and carbon dioxide. *Fuel*, 1983, **62**(2), 162–165.
6. Pan, L. W. *Study on the Pyrolysis Characteristics of Jimsar Oil Shale and the Theory and Simulation of Dry Distillation Furnace*. Ph.D. Thesis, Wuhan University of Science and Technology, 2017 (in Chinese).
7. Li, S. Y., Yue, C. G. Study of pyrolysis kinetics of oil shale. *Fuel*, 2003, **82**(3), 337–342.

8. Bar, H., Ikan, R., Aizenshtat, Z. Comparative study of the isothermal pyrolysis kinetic behaviour of some oil shales and coals. *J. Anal. Appl. Pyrolysis*, 1988, **14**(1), 49–71.
9. Wang, W., Li, S. Y., Li, L. Y., Ma, Y., Yue, C. T., He, J. L. Pyrolysis kinetics of North-Korean oil shale. *Oil Shale*, 2014, **31**(3), 250–265.
10. Wang, Q., Liu, H. P., Sun, B. Z., Li, S. H. Study on pyrolysis characteristics of Huadian oil shale with isoconversional method. *Oil Shale*, 2009, **26**(2), 148–162.
11. Vyazovkin, S., Chrissafis, K., Di Lorenzo, M. L., Koga, N., Pijolat, M., Roduit, B., Sbirrazzuoli, N., Sunol, J. J. ICTAC Kinetics Committee recommendations for collecting experimental thermal analysis data for kinetic computations. *Thermochim. Acta*, 2014, **590**, 1–23.
12. Pan, N., Yue, Y., He, Z., Lv, W. Influence of transition metal salts and pyrolysis conditions on the product yield via Jimsar oil shale pyrolysis. *Oil Shale*, 2020, **37**(4), 304–318.
13. Pan, N., Li, D., Lü, W., Dai, F. Q. Kinetic study on the pyrolysis behavior of Jimsar oil shale. *Oil Shale*, 2019, **36**(4), 462–482.